LOW-COST MAPPING OF FOREST UNDER-STOREY VEGETATION USING SPHERICAL PHOTOGRAMMETRY

A. Murtiyoso [1*], H. Hristova [2], N. Rehush [2], V.C. Griess [1]

[1] Forest Resources Management, Institute of Terrestrial Ecosystems, Department of Environmental Systems Science, ETH Zurich, Switzerland - (arnadi.murtiyoso, verena.griess)@usys.ethz.ch
[2] Swiss National Forest Inventory, Swiss Federal Institute for Forest, Snow and Landscape Research WSL, Switzerland – (hristina.hristova, nataliia.rehush)@wsl.ch

Commission II

KEY WORDS: low-cost, forest, under-storey, photogrammetry, spherical, 360° images

ABSTRACT

This paper is an attempt to respond to the growing need and demand of 3D data in forestry, especially for 3D mapping. The use of terrestrial laser scanners (TLS) dominates contemporary literature for under-storey vegetation mapping as this technique provides precise and easy-to-use solutions for users. However, TLS requires substantial investments in terms of device acquisition and user training. The search for and development of low-cost alternatives is therefore an interesting field of inquiry. Here, we use low-cost 360° cameras combined with spherical photogrammetric principles for under-storey vegetation mapping. While we fully assume that this low-cost approach will not generate results on par with either TLS or classical close-range photogrammetry, its main aim is to investigate whether this alternative is sufficient to meet the requirements of forest mapping. In this regard, geometric analyses were conducted using both TLS and close-range photogrammetry as comparison points. The diameter at breast height (DBH), a parameter commonly used in forestry, was then computed from the 360° point cloud using three different methods to determine if a similar order of precision to the two reference datasets can be obtained. The results show that 360° cameras were able to generate point clouds with a similar geometric quality as the references despite their low density, albeit with a significantly higher amount of noise. The effect of the noise is also evident in the DBH computation, where it yielded an average error of 3.5 cm compared to both the TLS and close-range photogrammetry.

1. INTRODUCTION

3D mapping as an extension of traditional surveys of forest environments has seen increasing interest in recent years. Reconstructing forests in 3D opens possibilities for various applications previously either impossible or difficult to do using traditional methods, such as individual tree mapping and geometry-based analyses. Serious consideration has therefore been given to integrating 3D mapping techniques for National Forest Inventories (NFI) (Kükenbrink et al., 2022). In parallel to this increase in demand, existing 3D mapping technologies have also evolved significantly, as can be seen in the use of various techniques such as terrestrial laser scanning (TLS) (Rehush et al., 2018) or mobile laser scanning (MLS) (Cabo et al., 2018) in forest mapping. Indeed, TLS remains the gold standard both in terms of precision and ease-of-use for this particular application (Kükenbrink et al., 2022), especially where under-storey vegetation is concerned. While parallel developments in aerial lidar acquisition have also seen significant improvements, especially in miniaturisation (Corte et al., 2020), assessing under-storey vegetation is used to answer very specific questions, which may only be addressed using data obtained via terrestrial techniques. This includes, for example, the monitoring of tree growth (Brolly et al., 2013) or tree microhabitats (Fol et al., 2022), for both of which the level of detail provided by aerial lidar is often insufficient simply due to occlusions in forests.

While laser scanning technology is currently the preferred solution for under-storey forest mapping, one of its main constraints is the cost. Indeed, the costs for lidar data acquisition has remained high in recent years thus often requiring researchers to choose between quality and budget in many financially constrained projects. A possible solution to this problem is the use of alternative 3D mapping techniques such as close-range photogrammetry and depth cameras (Fol et al., 2022). However, these solutions present users with another problem: notably the strictly convergent nature of photogrammetric acquisition networks. This constraint in close-range photogrammetry means that data acquisition is not practical in a complex and heterogeneous forest situation. Despite this fact, close-range photogrammetry has the potential to generate more detail than laser scans, as has been showcased in other applications (Fassi et al., 2011; Menna et al., 2018).

Depth cameras also presented interesting results, but their limited scope makes a large-scale implementation difficult. The novel solid-state lidar (SSL) technology - that can for example be found in recent Apple© iPads and iPhones come with the same advantages and inconveniences as depth cameras (Murtiyoso et al., 2021). Other low-cost solutions for forest mapping include the use of action cameras with fish-eye lenses as evidenced by Kükenbrink et al. (2022), but since fish-eye cameras still utilise photogrammetric concepts for the 3D reconstruction phase, again convergent networks are required, albeit to a lesser degree.

In this research, we investigated the potential of different low-cost technologies in 3D forest mapping. Spherical photogrammetry or the use of 360^0 images is not a new technology. Its use was studied for example by Fangi & Nardinocchi (2013), who described its use in the cultural heritage domain. Barazzetti et al. (2017) described the use of

* Corresponding author

360^0 degree images for 3D mapping, while their updated and more recent research detailed in Barazzetti et al. (2022) showcased how using recent types of panoramic cameras may yield impressive results in an urban setting. In the specific application of forest mapping, Hristova et al. (2022) implemented a deep-learning method to perform mapping based on monocular spherical images.

In this study, we attempted to apply multi-image spherical photogrammetry for this task. The main reasoning behind this idea is that the use of 360^0 cameras is easy, fast, and reasonably low-cost (more so when compared to the gold standard of TLS). The device is also very compact and light, and the collecting of videos does not require any additional equipment (e.g., a tripod). While in many aspects this means the use of 360^0 cameras is advantageous, one remaining research question to be answered is whether their picture quality, both geometric and radiometric, is enough for forest mapping purposes. As we are aware of the limitations of this low-cost alternative, the main objective of our experiments was not to compare it to TLS head-to-head, but rather to determine if its quality is sufficient when considering recent hardware and software as is available on the market. For this purpose, an *a priori* assumption of 1-2 cm precision will be considered as sufficient. This value was chosen based on the available precision for manual tree diameter measurement, a parameter of which was also derived from the point cloud and assessed in this paper.

2. MATERIALS AND METHODS

(a) (b)

Figure 1. Field setting for data acquisition: (a) automatic coded targets used and (b) the Ricoh Theta Z1 360° camera.

Data acquisition. For the purpose of this research, 360° videos were taken in the Rameren forest in Birmensdorf, Switzerland. An initial test of using 360° images was performed but yielded subpar results, mainly due to the difficulty of obtaining sufficient overlap between successive images in a forest environment. A Ricoh Theta Z1 panoramic camera (Figure 1) was used to obtain the 360° video using a 30 FPS rate, 4K resolution, and 7 mm focal length. For the dataset used in this paper, the panoramic videos were taken around one specific tree (dubbed "Tree 01") which contains several objects of interest such as microhabitats. Two 360° videos of around 15 seconds each were split using Agisoft Metashape, resulting in 246 frames thus ensuring sufficient overlap. The first video was obtained with the user facing the studied tree, the second one with the tree in their back. Metashape was also employed to perform external orientation by using its spherical camera model. Scaling was performed by detecting several coded-target (CT) pairs. Dense matching was thereafter performed to obtain the dense point cloud.

Figure 1 shows the type of CT used during data acquisition as well as the sensor deployed. For each CT pair, a constant distance of 13.3 cm between their centres serves as scaling factors for the photogrammetric project. These CT pairs were placed around the forest in both planar and vertical distribution in line with common aerotriangulation requirements. For the particular case of "Tree 01", four CTs were identified around the object (Figure 2), thus giving the project four scale bars. Note that the CT does not have georeferenced coordinates due to difficulties in performing topographical surveys in forests. The resulting point cloud will therefore be scaled but not georeferenced.

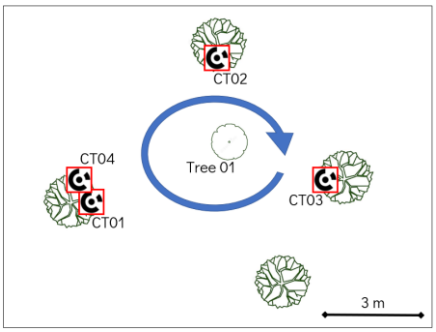

Figure 2. Situational top-down sketch of the dataset used in this paper with distribution of CT. The blue arrow indicates the direction of data acquisition.

In terms of geometrical analysis, two types of investigation were carried out to determine the geometric quality of the 360^0 dense point cloud. First, a comparison to datasets considered as having superior precision was made. This comparison uses a dataset of "Tree 01" acquired using the Leica BLK360 TLS and close-range photogrammetry. For the TLS dataset, four single scans with a "standard" resolution (circa 18 Mio. Points per scan) were collected. The scans were regularly distributed around the tree and resulting single point clouds were later co-registered in the Cyclone REGISTER 360 software. For the photogrammetric dataset, a Nikon Z50 18 mm was used to take convergent images which were then also processed using Metashape. Similarly to the 360° dataset, scaling was performed using the CT located around the object.

Point cloud analysis. The Multiscale Model to Model Cloud Comparison (M3C2) (Lague et al., 2013) plug-in of the software CloudCompare (https://www.danielgm.net/cc/ accessed 18 October 2022) was used in order to provide a robust error analysis between two point clouds. The M3C2 method generates a signed Euclidean distance between points from two point clouds by assuming a local surface.

The second analysis derived the diameter at breast height (DBH) of "Tree 01" from the three available point clouds. The DBH is a very important parameter from which various other forest-related values may be derived. It is traditionally defined as the diameter of the tree at a height of 1.3 m (Paul et al., 2017). To this end, a first step includes the determination of the ground level. This was done by using the Cloth Simulation Filter (CSF) method (Zhang et al., 2016). From the ground surface, a height of 1.3 m was measured and a cross-section at this height was taken for all three point clouds with a thickness of 10 cm. For DBH measurement purposes, these cross-sections were thereafter projected to the 2D space by first determining the principal vertical axis of the points using the Principal Component Analysis (PCA) method.

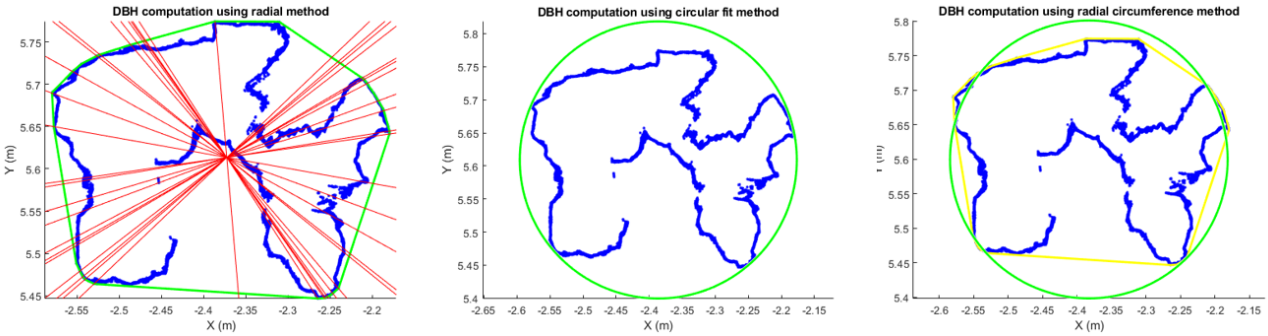

Figure 3. Illustration of the different methods for DBH computation using the cross-section of "Tree 01" at a 1.3 m height. The Nikon Z50 point cloud was used for this illustration.

Afterwards, three methods were proposed to simulate manual measurements of the DBH (Figure 3):

1. **Radial** method: to emulate the use of a calliper in manual DBH measurement, transversal sections of the projected cross-section were made using the centroid and each point in the point cloud. A convex-hull was also generated. The distance between the intersections between each transversal section and the convex-hull presents one DBH value. Using this method, there will be as many DBH values as the number of points in the point cloud. The final DBH value is therefore obtained from averaging these values.
2. **Circular** method: a simple least-squares circle-fitting algorithm was employed on the point cloud of the cross-section. The diameter of the fitted circle is thereafter taken as the DBH value. This method follows a similar approach, albeit simplified, taken by Pérez-Martín et al. (2021) in which the authors performed circle and cylinder fitting using RANSAC, Monte Carlo, and Optimal Circle methods. However, in our implementation a constraint was added in which the fitted circle must include all points inside it.
3. **Circumference** method: for this method, a convex hull was also computed for the cross-section. However, the total length of the convex hull was then considered as the value of the circumference of a circle. The DBH was then computed using these assumptions. This method attempts to emulate the use of a diameter tape, an alternative to callipers also commonly used in manual DBH measurements.

3. RESULTS AND DISCUSSIONS

Visually, the proposed technique already showed promising results to map under-storey vegetation (Figure 4). A quick look at the different scale bars (4 in total) used in the scene showed a scaling precision of 3.4 cm with two properly placed scale bars, while the remaining two check-distances yielded an overall accuracy of 1.7 cm. Note that these values indicate the overall quality of the photogrammetric project, i.e., internal and external orientation of the 246 input images. For the result to be useful in forest mapping, the dense point cloud generated using Metashape's dense matching function was also evaluated. To do so, the dense point cloud was compared to that of TLS and close-range photogrammetry, two solutions considered more precise than the 360° camera.

A common zone from the three point clouds was cropped so that the datasets are comparable in terms of area coverage. Noisy objects such as leaves from surrounding trees were also filtered using distance-based noise filtering, which does not suppress noisy points located near the main object itself (Figure 6).

Figure 4. Dense point cloud from the 360^0 video for the studied tree ("Tree 01") and its environment.

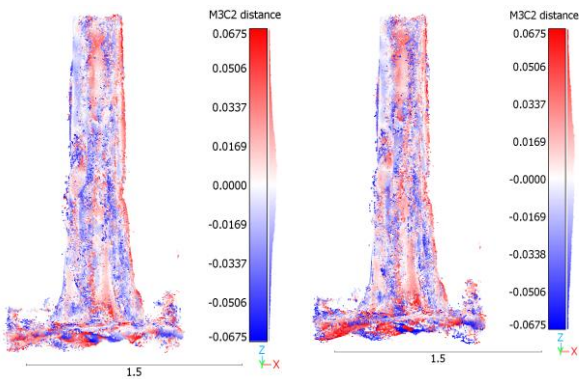

Theta Z1 vs. BLK 360
$\bar{x}$ = 0.1 cm; σ = ± 2.6 cm

Theta Z1 vs. Nikon Z50
$\bar{x}$ = 0.1 cm; σ = ± 2.9 cm

Figure 5. M3C2 analysis of the Theta Z1 point cloud, compared to TLS and close-range photogrammetry.

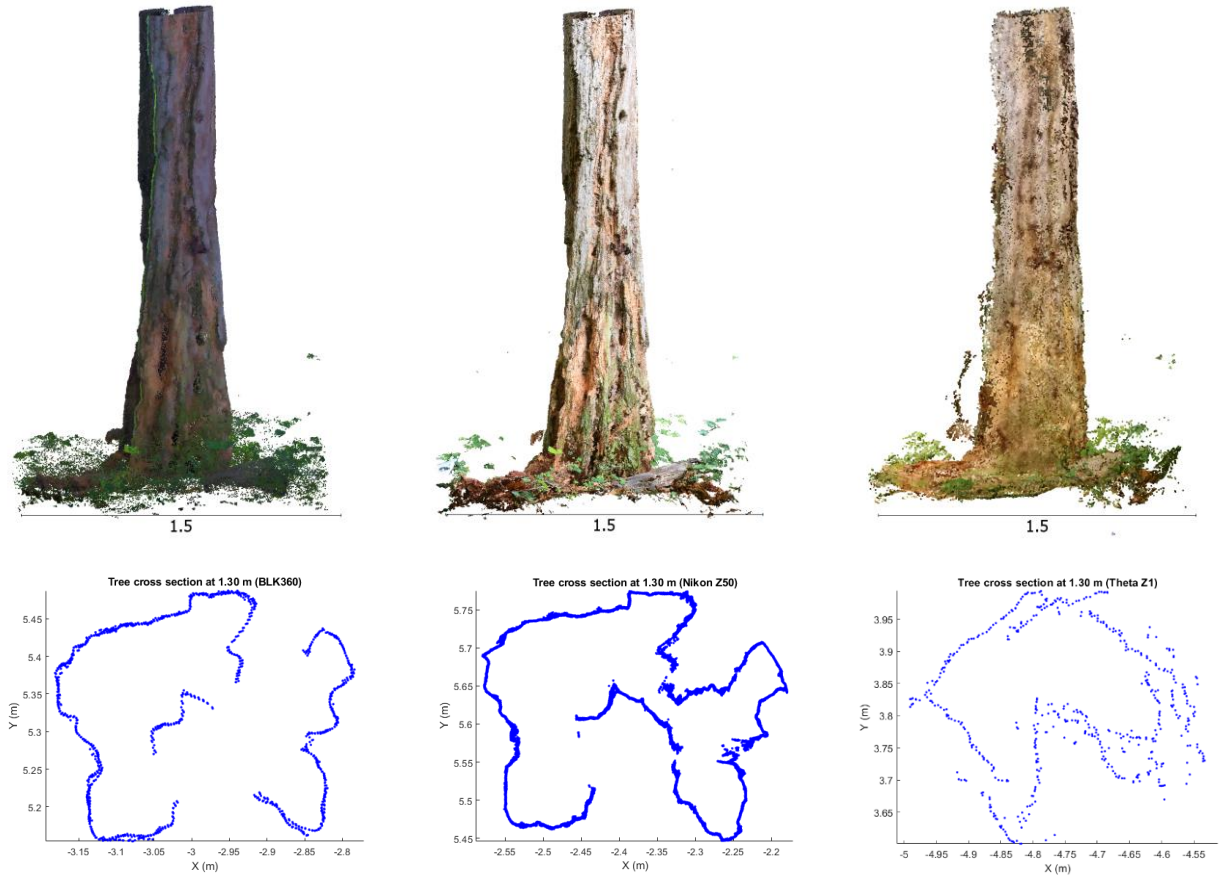

Figure 6. Cleaned dense point cloud of "Tree 01" generated by (a) BLK360 TLS, (b) close-range photogrammetry using Nikon Z50, and (c) spherical photogrammetry using Ricoh Theta Z1. The lower figures show the respective cross-sections at a 1.3 m height and 10 cm thickness used for the DBH computation analysis.

Method	BLK360	Nikon Z50	Theta Z1
Radial	37.5 cm	37.2 cm	40.2 cm
Circular fit	42.1 cm	41.9 cm	46.7 cm
Circumference	38.7 cm	38.5 cm	41.5 cm

Table 1. Comparison of DBH from three 3D methods using different computation strategies.

As explained in Section 2, a first analysis was conducted by performing the M3C2 distance computation. For this purpose, the Ricoh Theta Z1 point cloud was independently compared to the TLS and Nikon Z50 data, thus yielding two comparisons as can be seen in Figure 5. The results are favourable since in both cases an average residual error of 1 mm was obtained. However, the standard deviation of 2.6-2.9 cm indicates the presence of considerable dispersion in the data. The error indicated a normal Gaussian distribution.

Indeed, as may be ascertained from Figure 6, this is confirmed visually by the Theta Z1 dense point cloud which presented a noisier data compared to both references. However, assuming an a priori precision of 1 cm in the point cloud data, this value of standard deviation is still within the limits of a 3σ tolerance.

The second analysis consisted of the determination of the DBH from "Tree 01", and was performed on all three acquisition techniques using the three methods described in Section 2. Table 1 and Figure 8 show the DBH based on the different datasets.

TLS and close-range photogrammetry gave similar values (Table 1), which agrees with previous studies (e.g., Kükenbrink et al. 2022). The average difference between these two methods is 2 mm, which – considering the *a priori* precision of 1 cm – may be considered negligible. In order to assess the quality of the 360° point cloud, the DBH values of TLS and close-range photogrammetry were averaged. Using this point of reference, Theta Z1 yielded an average error of 3.5 cm.

The largest error (4.7 cm) was observed for the circular method of computation. Indeed, from Figure 8 it may be surmised that the circle does not represent the form of the tree cross-section very well. In the case of the Theta Z1, the presence of noise near to the main body of the object also played a role in generating error. Note that for the purpose of the DBH computation, the point cloud cross-section already underwent a prior second noise filtering to delete point outliers located near the tree bodies.

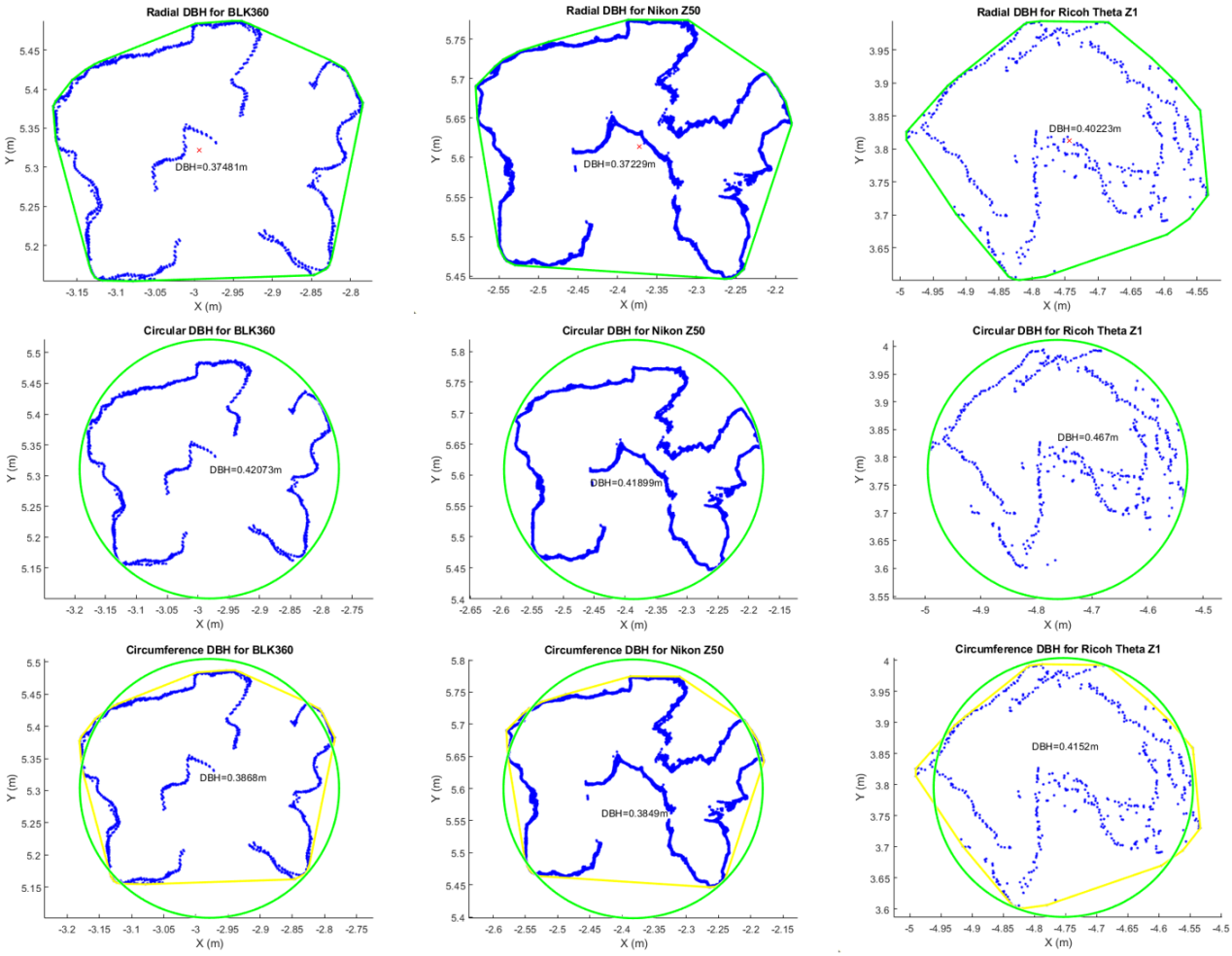

Figure 8. DBH computation using three different methods employed on the three different datasets.

As regards to comparison between the DBH computation methods, the radial and circumference methods (respectively emulating the calliper and diameter tape manual measurements) gave similar values. The average difference of the two methods across the three datasets was 1.3 cm, which falls very well within the tolerance. The circular method yielded the largest difference to the other two approaches with an average difference of 4.6 cm. The use of a circle fitting algorithm which must encompass all points in its interior may have been the main reason to this observation.

4. CONCLUSIONS

The paper presented the use of 360° camera and spherical photogrammetry to perform the 3D mapping of a forest environment. In this study, the quality of the proposed technique was assessed in the case of a single tree as an initial proof of concept. From a photogrammetric point of view, the proposed method achieved satisfactory results in terms of scaling precision (3.4 cm) and check accuracy (1.7 cm). In a future application involving a much larger area e.g., a forest plot, placing evenly spread scale bars must be an important consideration. Their distribution should not only be optimized horizontally, but also vertically, since the method works in the 3D space. The use of the proposed CT pairs worked quite well to perform the scaling since its use permitted automatic target identification and therefore saves a lot of time during the processing stage.

Out of the photogrammetric network, a dense point cloud was also generated. This point cloud was then compared to two references: namely TLS and close-range photogrammetry. The choice of these two references is based on the fact that close-range photogrammetry provided the best precision for a point cloud at this scale, but a TLS is already very precise for forest purposes, more practical to deploy, and can be considered the current standard in 3D forest mapping. Our results show that for the single trees, TLS and close-range photogrammetry shows negligible differences. The 360° point cloud also compared favourably in terms of overall geometric quality compared to both references. A more detailed analysis involving the computation of DBH showed that it attained an average difference of 3.5 cm from the reference. This value may indicate that the method is still acceptable for simple mapping, particularly for the computation of DBH.

Three methods for DBH computation were also tested in this study. Of these three, the radial and circumference methods produced very similar results while the circular method presented the most discrepancy. Further investigations using more data from other trees and a comparison to traditional DBH measurement techniques may be interesting future avenues of research to pursue. Such comparisons may start discussions on the precision of manual and digital methods and whether a digital method is valid alternative to traditional manual measurements, both in terms of precision and cost.

The main caveat of the presented results is that they were obtained for a single tree only. A larger scale analysis of a similar nature is already envisaged to present a statistically significant conclusion on this matter. Nevertheless, based on this case study the use of 360° cameras in 3D forest mapping showed a strong and promising potential as a low-cost alternative to TLS. Other than the simple computation of DBH, the technique may also be used to assess other forest characteristics (e.g., forest structure) which may not require a very precise point cloud.

Considering firstly that the cost of the device is a fraction of most TLS in the market and secondly that data acquisition is very quick (as opposed to e.g., close-range photogrammetry), the attained results show great promise. The acquisition of 360° videos in this case also follows the same general guidelines to basic TLS operation. In the longer term, these comparisons will serve as benchmark data guiding stakeholders in choosing the appropriate method for their forest mapping purposes, including national forest inventories.

ACKNOWLEDGEMENTS

The authors would like to thank Cyprien Fol and Daniel Kükenbrink for sharing their TLS and close-range photogrammetry datasets. We would also like to thank Michel Scheggia for his help in developing the various digital DBH measurement methods.

REFERENCES

Barazzetti, L., Previtali, M., & Roncoroni, F. (2022). 3D Modeling With 5K 360° Videos. International Archives of the Photogrammetry, Remote Sensing and Spatial Information Sciences - ISPRS Archives, 46(2/W1-2022), 65–71. https://doi.org/10.5194/isprs-archives-XLVI-2-W1-2022-65-2022

Barazzetti, L., Previtali, M., & Roncoroni, F. (2017). 3D modelling with the samsung gear 360. International Archives of the Photogrammetry, Remote Sensing and Spatial Information Sciences, XLII-2/W3, 85–90. https://doi.org/10.5194/isprs-archives-XLII-2-W3-85-2017

Brolly, G., Király, G., & Czimber, K. (2013). Mapping forest regeneration from terrestrial laser scans. Acta Silvatica et Lignaria Hungarica, 9(1), 135–146. https://doi.org/10.2478/aslh-2013-0011

Cabo, C., Del Pozo, S., Rodríguez-Gonzálvez, P., Ordóñez, C., & González-Aguilera, D. (2018). Comparing terrestrial laser scanning (TLS) and wearable laser scanning (WLS) for individual tree modeling at plot level. Remote Sensing, 10(4). https://doi.org/10.3390/rs10040540

Corte, A. P. D., Rex, F. E., de Almeida, D. R. A., Sanquetta, C. R., Silva, C. A., Moura, M. M., Wilkinson, B., Zambrano, A. M. A., da Cunha Neto, E. M., Veras, H. F. P., de Moraes, A., Klauberg, C., Mohan, M., Cardil, A., & Broadbent, E. N. (2020). Measuring individual tree diameter and height using gatoreye high-density UAV-lidar in an integrated crop-livestock-forest system. Remote Sensing, 12(5). https://doi.org/10.3390/rs12050863

Fangi, G., & Nardinocchi, C. (2013). Photogrammetric processing of spherical panoramas. Photogrammetric Record, 28(143), 293–311. https://doi.org/10.1111/phor.12031

Fassi, F., Achille, C., & Fregonese, L. (2011). Surveying and modelling the main spire of Milan Cathedral using multiple data sources. The Photogrammetric Record, 26(136), 462–487.

Fol, C. R., Murtiyoso, A., & Griess, V. C. (2022). Evaluation of Azure Kinect Derived Point Clouds To Determine the Presence of Microhabitats on Single Trees Based on the Swiss Standard Parameters. International Archives of the Photogrammetry, Remote Sensing and Spatial Information Sciences - ISPRS Archives, 43(B2-2022), 989–994. https://doi.org/10.5194/isprs-archives-XLIII-B2-2022-989-2022

Hristova, H., Abegg, M., Fischer, C., & Rehush, N. (2022). Monocular Depth Estimation in Forest Environments. International Archives of the Photogrammetry, Remote Sensing and Spatial Information Sciences - ISPRS Archives, 43(B2-2022), 1017–1023. https://doi.org/10.5194/isprs-archives-XLIII-B2-2022-1017-2022

Kükenbrink, D., Marty, M., Bösch, R., & Ginzler, C. (2022). Benchmarking laser scanning and terrestrial photogrammetry to extract forest inventory parameters in a complex temperate forest. International Journal of Applied Earth Observation and Geoinformation, 113(March), 102999. https://doi.org/10.1016/j.jag.2022.102999

Lague, D., Brodu, N., & Leroux, J. (2013). Accurate 3D comparison of complex topography with terrestrial laser scanner: Application to the Rangitikei canyon (N-Z). ISPRS Journal of Photogrammetry and Remote Sensing, 82, 10–26. https://doi.org/10.1016/j.isprsjprs.2013.04.009

Menna, F., Nocerino, E., Drap, P., Remondino, F., Murtiyoso, A., Grussenmeyer, P., & Börlin, N. (2018). Improving underwater accuracy by empirical weighting of image observations. International Archives of the Photogrammetry, Remote Sensing and Spatial Information Sciences - ISPRS Archives, 42(2). https://doi.org/10.5194/isprs-archives-XLII-2-699-2018

Murtiyoso, A., Grussenmeyer, P., Landes, T., & Macher, H. (2021). First assessments into the use of commercial-grade solid state lidar for low cost heritage documentation. International Archives of the Photogrammetry, Remote Sensing and Spatial Information Sciences - ISPRS Archives, 43(B2-2021), 599–604. https://doi.org/10.5194/isprs-archives-XLIII-B2-2021-599-2021

Paul, K. I., Larmour, J. S., Roxburgh, S. H., England, J. R., Davies, M. J., & Luck, H. D. (2017). Measurements of stem diameter: implications for individual- and stand-level errors. Environmental Monitoring and Assessment, 189(8). https://doi.org/10.1007/s10661-017-6109-x

Pérez-Martín, E., Medina, S. L. C., Herrero-Tejedor, T., Pérez-Souza, M. A., de Mata, J. A., & Ezquerra-Canalejo, A. (2021). Assessment of tree diameter estimation methods from mobile laser scanning in a historic garden. Forests, 12(8). https://doi.org/10.3390/f12081013

Rehush, N., Abegg, M., Waser, L. T., & Brändli, U. B. (2018). Identifying tree-related microhabitats in TLS point clouds using machine learning. Remote Sensing, 10(11), 1–23. https://doi.org/10.3390/rs10111735

Zhang, W., Qi, J., Wan, P., Wang, H., Xie, D., Wang, X., & Yan, G. (2016). An easy-to-use airborne LiDAR data filtering method based on cloth simulation. Remote Sensing, 8(6), 1–2